



EXODUS

Paula Benitez, Mark Boyd, Citlali Bruce Rosete, Wiebe de Griijter, Johan Frich,
Liana Gfrerer, Jan-Vincent Harre, Kim Angelique Kahle, Mireia Leon Dasi,
Gerald Möslenlechner, Johannes Ora, Vito Saggese, Eleftheria Sotiriou,
Marco Souza de Joode, Apostolos Gunnari Symeonidis, Laszlo Talaber

Engineering tutor: Günter Kargl

Science tutor: Leonard Schulz

July 19, 2023

Abstract

EXODUS is a single-telescope proposed mission to study the largely unexplored range of sub-Neptune to Jupiter sized exoplanets on orbital periods over 100 days. The focus of the mission lies in detection of these planets and to characterise atmospheric escape to constrain their evolutionary pathway. Further, the activity of the host star will be monitored in the UV to distinguish two mechanisms of atmospheric escape: UV-driven mass loss and core-powered mass loss. We propose a space telescope on an L_2 orbit that can spectroscopically resolve exoplanets in the NIR using a coronagraph, while simultaneously observing the star with a UV photometer.

1 Introduction

Over the last 25 years, thousands of exoplanets have been detected, providing us with a first glimpse into the vast population of exoplanets that are expected to orbit the stars. The distribution of currently detected planets is heavily skewed to short orbital periods (< 100 days), due to the observational biases of existing detection methods. As a consequence, our knowledge of planets on long orbital periods is limited, both in terms of their demographics and their evolution.

From the sample of exoplanets on short orbital periods, we can make inferences about trends in the population. Notably, planets with orbital periods less than 100 days follow a bimodal radius distribution, with a dip in the occurrence rate of planets with $2.3 R_{\text{Earth}}$, known as the radius valley (Fulton et al., 2017).

A possible explanation of this radius valley is atmospheric escape (see e.g., Owen & Wu, 2013). In this process, planets with a large fraction of their mass in the atmosphere lose the atmosphere and shrink in the process, which leads to the two peaks in the radius distribution. Atmospheric escape has been detected for planets on short orbital periods (Spake et al., 2018a), but no detections exist for planets on long orbital periods. It is an open question whether atmospheric escape is relevant to the evolution of planets on long orbital periods, and what the radius distribution for these planets is.

The architecture of our solar system raises further questions as to the demographics of long orbital period planets.

The solar system is unusual for the fact that it contains neither a super-Earth nor a sub-Neptune, the two most commonly occurring planets on low orbital periods. The outer planets are Neptune size and above, but it is unknown whether this characteristic is a peculiarity among planetary systems or whether the solar system is a common system in this regard. Finally, it is also unclear whether the solar system architecture, with inner rocky planets and outer giants, is common among planetary systems.

These questions call for new detection methods to fill in the gap of planets on long orbital periods with Neptune radii and below. This will allow us to determine whether our solar system is unique or not, placing it in the wider context of planetary systems. Moreover, it will enable us to further constrain the ingredients required for habitable planets to form.

1.1 Mission profile

The EXODUS mission targets both the detection and characterisation of exoplanets on long-period (>100 days) orbits. The first phase will be dedicated to revisiting previously detected target objects for probing the presence of atmospheric escape based on the metastable He 1083 nm transition (Oklopčić & Hirata, 2018). These observations are complemented with UV monitoring of the host-star, allowing for a correlation between atmospheric escape and stellar activity after multiple revisits of the systems.

The second mission phase will expand the observations to a survey of stars with known short-period exoplanets,

aiming to detect long-period counterparts in the stellar systems. The planetary parameters derived from these observations will reduce the current observational bias on planet detections. This will clarify further how the architecture of the solar system relates to the structure of other stellar systems.

The mission objective is achieved with a detector system that combines a UV photometer for star monitoring with a coronagraph spectrometer operating in the near infrared for directly imaging the planets. Complex adaptive objects in the instrument further improve the contrast, enabling us to target planets with contrasts as low as 10^{-9} .

1.2 Previous and future missions

There have been several ground and space-based missions aiming at discovering the diversity of extrasolar planets. Besides radial velocity measurements of stars with detectors like HARPS (Mayor et al., 2003) and ESPRESSO (Pepe et al., 2021), photometric observations were carried out to detect planets during transit in front of their host stars. In this regard, ground-based surveys from e.g. the Wide Angle Search for Planets (WASP) project (Pollacco et al., 2006) and Next-Generation Transit Survey (NGTS) (Wheatley et al., 2018) found many large and close-in exoplanets.

Space-based observatories aimed at the discovery and characterisation of exoplanets include CoRoT (Convection Rotation and planetary Transits, Auvergne et al. (2009)), Kepler (Borucki et al., 2010), Transiting Exoplanet Survey Satellite (TESS), Ricker et al. (2015a), and characterising ExOPlanets Satellite (CHEOPS), Benz et al. (2021)). All of these contributed to the sample of known exoplanets, and delivered a few targets towards our science goals.

The Gaia space mission (Gaia Collaboration et al., 2016) is mainly aimed at astrometric measurements of stars to discover exoplanets. The James Webb Space Telescope (JWST) (Gardner et al., 2006) is being aimed at, amongst other things, characterising atmospheres. Both of these could also provide some targets towards our science case. Future space missions like PLANetary Transits and Oscillations of stars (PLATO), Rauer et al. (2014) and the Nancy Grace Roman Space Telescope (Spergel et al., 2015) are expected to discover Neptune-sized planets with orbital periods of more than 100 days.

Furthermore, Ariel (Tinetti et al., 2018) will utilize transmission spectroscopy to analyze the atmospheres of about 1000 exoplanets, possibly including the detection of atmospheric escape. However, due to the limitations of the transit method, the Ariel targets are constrained to relatively short periods.

One proposed future mission, which is yet to be confirmed, is the Habitable Worlds Observatory (HWO). It aims to directly image Earth-sized planets and probe their atmospheres. See LUVUOIR (The LUVUOIR Team, 2019) and Habex (Gaudi et al., 2020) for proposed capabilities.

2 Science Case

2.1 Key science questions & objectives

Our proposed space mission, EXODUS, aims to study the evolution of exoplanets and the architecture of their parent

systems.

In that regard, our first question (Q1, Table 1) addresses the topic of atmospheric escape. There are two main hypotheses to explain this process. The first is UV-driven mass loss, in which UV flux from the host star heats up the upper layer of the atmosphere. As a consequence, its thermal energy exceeds the gravitational binding energy of the planet, and the atmosphere flies off into free space (Lammer et al., 2003). An alternative explanation is core-powered mass loss, in which remnant heat of planet formation leads to hydrodynamic escape (Ginzburg et al., 2018). These two models are degenerate since they can both explain the observed distribution of planets. The presence of Helium in the exosphere is a probe to measure atmospheric escape (Oklopčić & Hirata, 2018). In the exosphere, Helium exists in a metastable triplet state, creating an absorption line at 1083 nm. This absorption signature has been used to directly detect atmospheric escape (Spake et al., 2018b).

With EXODUS, we may examine whether the radius valley also exists for long-period planets or whether this is just a feature of short-period exoplanets. Investigating the radius valley through atmospheric escape will improve our understanding of planetary evolution and, consequently, our own solar system.

The second question (Q2 in Table 1) addresses the inherent bias of exoplanet detection techniques. Especially, the discovery of long-period exoplanets is limited by the transit and radial velocity methods, which have contributed the most to the sample of known exoplanets. Through new detections via direct imaging with EXODUS, we may fill the relatively unexplored region in the period-mass diagram (see Figure 1). Furthermore, EXODUS may confirm planetary parameters for both new discoveries and exoplanet candidates through dedicated follow-up observation.

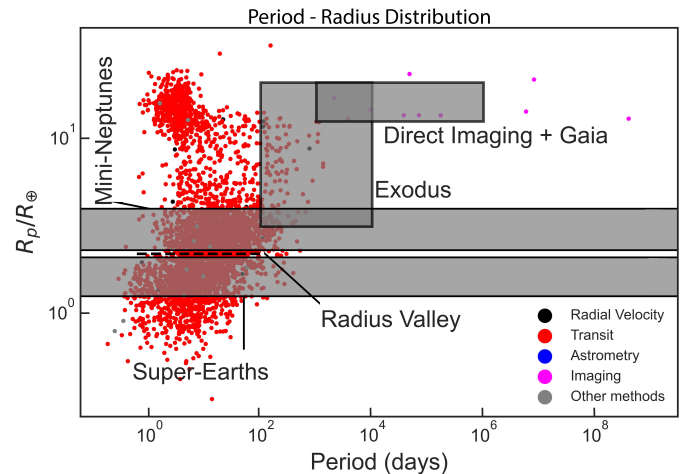


Figure 1: The orbital period - radius diagram for exoplanets discovered by different methods.

EXODUS will enable the improved demographic characterisation of planetary systems from which we may infer to what extent our solar system is unique. This science question is addressed by Q3 in Table 1. By identifying large planets with long orbital periods, we may find analogues to the ice giants of our solar system, hence decreasing the likelihood of a unique structure. Furthermore, the search for mini-Neptunes on long-period orbits may answer the question of why the solar system is lacking an analogous

planet.

2.2 Science requirements

In order to answer our above stated science questions and to fulfill our science objectives, we derived the following science requirements:

- SCI1: The mission design shall allow for the detection of atmospheric escape through direct observation of the He triplet at 1083 nm in reflected light.
- SCI2: The mission design shall allow for the measurement of the stellar activity of host stars in UV.
- SCI3: The mission design shall allow separation of single planets in multi planet systems.
- SCI4: The mission design shall allow the observation of exoplanets with a minimum radius of 3 Earth radii.
- SCI5: The mission design shall allow the observation of exoplanets with a minimum orbital period of greater than 100 days.
- SCI6: The mission design shall allow the observation of A to M stellar types.
- SCI7: The mission shall allow observations to be carried out for a core sample of 5000 exoplanets.

2.3 Observation Requirements

In order to reach our scientific objectives, we chose the following observation requirements:

- OBR1: The mission design shall allow direct, spatially resolved spectroscopy of the exoplanetary system in NIR (1000-1500 nm).
- OBR2: The mission design shall allow for the simultaneous photometric measurement of the UV flux of the host star.
- OBR3: The mission design shall allow for the detection of exoplanets with contrast ratios of 10^{-9} .
- OBR4: The mission design shall allow the observation of exoplanets at an angular separation range of at least 0.17 arcsec from their host star.
- OBR5: The mission design shall allow for spectrophotometry to be carried out for exoplanet systems with a distance of up to 100 pc from the Earth.
- OBR6: The spacecraft shall provide spectroscopy measurements with $\text{SNR} \geq 5$.

2.4 Mission requirements

The mission requirements, which are derived from the science and observation requirements, are presented in the following. The final traceability matrix is shown in Fig. 2

- MR1: The mission design shall allow for the observation of the target sample within 5 years.
- MR2: At least 30% of the sky shall be observable at all times.
- MR3: The spacecraft shall ensure that the angle to the Sun never exceeds $\pm 10^\circ$ (x -axis), $\pm 22^\circ$ (y -axis), and -10° and 20° (z -axis).
- MR4: The final orbit shall be a Lissajous orbit around Lagrange point L_2 .

	SO-1	SO-2	SO-3	SCI-01	SCI-02	SCI-03	SCI-04	SCI-05	SCI-06	SCI-07	OBR-02	OBR-03	OBR-05	OBR-06	MIS-01	MIS-02
SCI-01																
SCI-02																
SCI-03																
SCI-04																
SCI-05																
SCI-06																
SCI-07																
OBR-01																
OBR-02																
OBR-03																
OBR-04																
OBR-05																
OBR-06																
MIS-01																
MIS-02																
MIS-03																
MIS-04																

Figure 2: Traceability matrix of the requirements and objectives.

3 Payload

3.1 Telescope

The chosen telescope is of an elliptical off-axis Korsch design with a focal length of $f = 133$ m. It consists of 4 mirrors before the collected light is diverted to the instrument bay where it is split into different bands. The first mirror (M1) is an elliptical mirror with the dimensions $4.4 \text{ m} \times 3.5 \text{ m}$ and area of 12.09 m^2 , the second mirror (M2) is an elliptical mirror of dimensions $0.6 \text{ m} \times 0.44 \text{ m}$ with an area of 0.21 m^2 . The third mirror (M3) is an elliptical mirror $0.2 \text{ m} \times 0.18 \text{ m}$ and with an area of 280 cm^2 . The fourth mirror is a planar mirror with a diameter of 0.1 m and an area of 78 cm^2 . This mirror is a fast steering mirror (FSM) which provides the finesse for pointing precisely to distant objects.

The elliptical mirrors were chosen to maximize the photon count. The off-axis design was chosen to maximize image contrast, which is one of the main system drivers.

3.2 Optical system

Inside the telescope’s focal plane assembly (see Figure 3), a dichroic (DF1) splits the light according to wavelength and distributes it between the science instruments of EXODUS: the Coronagraph and Integral Field Unit, MARY, and the UV and visual photometer, UVIS.

3.2.1 MARY: The vector coronagraph and integral field unit.

The near-infrared (NIR) branch from DF1 consists of the Adaptive Optics (AO) segment and the MARY system. The payload requirements on MARY place strict requirements on the AO.

The wavefront, distorted by minute deviations caused by thermal and other stresses in M1, M2, and M3, is fed to the AO system, which comprises of 3 deformable mirrors (DMs), forming conjugate pairs (M1 – DM1, M2 – DM2, M3 – DM3). Each DM is a thin, elliptical mirror with dimensions corresponding to the dimensions of the telescope exit pupil. In today’s AO systems, the number M of actuators placed on the back of the DM is $M > N$ (Brož et al.,

Table 1: Scientific questions and objectives of the EXODUS mission.

Science Questions	Science Objectives
Q1. How does atmospheric escape shape the evolution of long orbital period exoplanets?	O.1. Characterisation O1.1. Distinguish the physical processes responsible for atmospheric escape, namely stellar UV flux and core-powered mass loss. O1.2. Determine the magnitude of atmospheric escape on exoplanets, with respect to orbital period, planet radius and stellar type. O1.3. Establish whether or not the radius valley exists for long orbital period planets.
Q2. What proportion of the exoplanet population do giant planets with long orbital periods represent?	O.2. Detection O2.1. Update the period-radius diagram with detections of giant planets on long orbital periods.
Q3. How does the solar system architecture compare to that of exoplanetary systems?	O.3. Contextualisation O.3.1. Establish the occurrence rate of systems with inner rocky planets and outer giant planets. O.3.2. Establish whether sub-Neptunes exist on long period orbits.

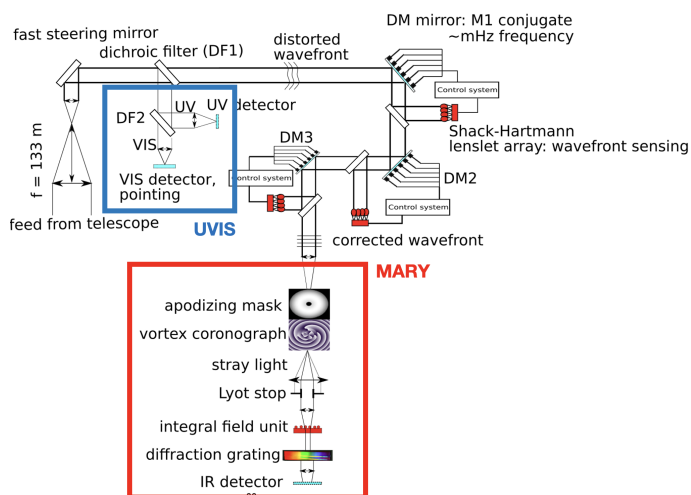


Figure 3: A diagram of the optical path, with the MARY and UVIS instruments marked in red and blue, respectively.

2017), where N is the highest order of the Zernike polynomial (Zernike, 1934), which are needed to correct the wavefront. Deformations of an elliptical mirror are described by Generalized Zernike polynomials (Navarro et al., 2014), which are a set of orthogonal polynomials parametrized by the eccentricity of the ellipse. Such a system has a low Technology Readiness Level (TRL).

To complete each one of the 3 AO loops, a beam-splitter and a Shack-Hartmann lenslet array (Platt & Shack, 2001) for wavefront sensing is necessary. The image data from the wavefront error sensor is analyzed by the control loop and a corresponding output is fed to the actuators.

The MARY instrument is the main science instrument of the spacecraft. It consists of an apodized elliptical vector vortex coronagraph and an integral field unit (IFU) equipped with a NIR detector. The apodizing mask greatly aids to achieve the required contrast of 10^{-9} . The transmission ratio of the apodizing mask is 68% (Guerri et al., 2011). The elliptical vector vortex coronagraph has 6π phase turn to achieve $0.17''$ inner working angle (IWA) based on observational requirements (OBR-04). This com-

ponent has a TRL of 2 and therefore requires a longer development time. Theoretical studies on such an instrument have been performed (Ruane & Swartzlander, 2013). A Lyot stop (Lyot, 1939) is required to block stray light.

An IFU based on the JWST NIRSpec instrument (Bagnasco et al., 2007) is used to obtain spatially resolved full-frame spectra. These are measured by the NIR Teledyne Hawaii 4RG sensor and fed to the OBC and are one of our principal data products.

The Mary instrument will be equipped with a single Teledyne HAWAII 4RG. This will allow the instrument to cover the required wavelength range without any gaps caused by mosaic arrangements. The detector was chosen for its favorable noise behavior and high quantum efficiency in the near-infrared. The detector will be controlled by the MARY Control Electronics (MCU), which contains the electrical interfaces for the detector, the DCU, a nominal and redundant DPU, and the nominal and redundant PSU. The processor for the MCU will be a Gaisler GR740, which will be sufficient to provide the processing of the large frames produced by Mary and the calculations for the adaptive optics systems. The MCU volatile memory is sized for full frame processing of science frames and the inputs of the Shack-Hartman wavefront sensors. This leads to a size of 256 MBytes. The non-volatile memory of the MCU needs to be 16 MBytes in order to store the software images, calibration data, and detector firmware.

The M4 telescope mirror is a planar fast steering mirror (FSM) used to increase the precision of the pointing of the telescope by performing fast tilt-shift corrections on the collimated beam. This tilt-shift correction aids the main AO system, which precedes the main instrument.

3.2.2 UVIS

UVIS is a combination of a UV Photometer and a visual Fine Guidance Sensor. This requires another dichroic inside of the optical path that distributes the light into these two channels.

The main scientific part of UVIS is the UV channel. This side measures the UV Flux of the target star to observe its activity while MARY observes the spectra of exoplanets. The sampling rate of the UVIS UV channel is dictated by

the flux of the target star in order to allow for the best scientific measurements possible.

The visual channel of UVIS is used as an input to the spacecraft attitude control system and operates at a rate of 10 Hz. The images obtained by the visual channel are used for target acquisition after a slew and fine guiding using the FSM of the telescope.

There are two main options for the detectors used by the UVIS. The first option represents the worst case with respect to performance and is based on the currently available technology. The detectors used in this baseline are a Teledyne CCD272-64 for the UV channel and a Teledyne CCD250-82 for the visual guiding channel. Both detectors provide the needed size of at least 2000 by 2000 pixels and a pixel pitch that is ideal for the tasks of the UVIS. The second option would use two Teledyne LACera CMOS detectors. This type of detector provides a better quantum efficiency in the UV range, which would be ideal for our measurement. However, this technology is not yet qualified for use in space.

The electrical system of UVIS consists of a nominal and redundant Data Processing Unit (DPU), a nominal and redundant Power Supply Unit (PSU), a Detector Control Unit (DCU) for each detector, and the cold and warm Front End Electronics (FEE) needed to interface with the detectors. The DPU will be equipped with a Gaisler GR712RC processor, which will provide the necessary processing power for guiding calculations and science data processing. The volatile memory is 64 KByte, which is enough to buffer science frames for further processing. The non-volatile memory will fit 8 Kbyte, which is needed for Software images, firmware, and calibration data.

3.3 Communications

The spacecraft will have three antennas. One of them will work in the X-band for science downlink with a data rate of 10 Mbps and another two in the S-band for housekeeping with a data rate of 4 kbps. The latter two are positioned so that if the spacecraft starts to tumble, it will be able to connect to a ground station anyway. The primary antenna is a 30.4 dB high gain antenna with 40 W of transmitting power and steering possibility for better science downlink speeds.

4 Mission Analysis

4.1 Launch and orbit

As shown in Figure 4, EXODUS will orbit Lagrange point L_2 in order to obtain a sufficiently low operational temperature and ensure the possibility of relatively long exposures. Specifically, a Lissajous orbit with a large amplitude was selected - similar to that of the Herschel space telescope. This orbit may be reached directly with the Ariane 62 launcher (Hechler & Yanez, 2004), which reduces the Δv to be provided by the spacecraft. The Ariane 62 launcher is able to deliver 3300 kg to orbit around L_2 (Lagier, 2021). As the wet mass of EXODUS is 2386 kg, Ariane 62 fulfills the launch and transfer requirement with a comfortable margin.

Table 2 shows the Δv budget for EXODUS. In the case that the 50 m s^{-1} allocated for the removal of launcher dis-

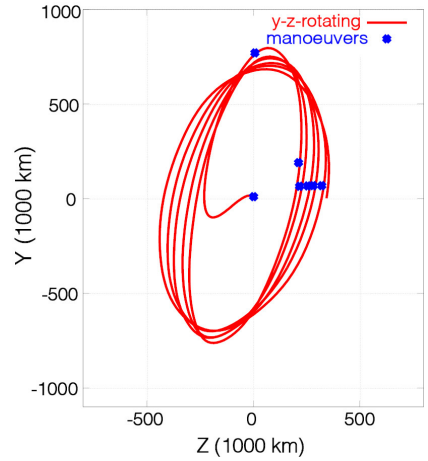


Figure 4: Lissajous orbit around the Lagrange point L_2 including the transfer from Earth. Figure adapted from Hechler & Yanez (2004).

Table 2: Δv budget of the mission.

L_2 injection contingency	50 m s^{-1}
Stationkeeping	25 m s^{-1}
Decommissioning	10 m s^{-1}
Total	85 m s^{-1}
Total with margin	128 m s^{-1}

person is not used, the mission lifetime may be increased. Furthermore, Table 2 reflects how the L_2 Lissajous orbit requires relatively small Δv for stationkeeping. Furthermore, the chosen orbit may be designed to avoid the eclipse of the Earth for 6 years, ensuring stable operating conditions for instruments and electronics (Hechler & Yanez, 2004).

4.2 Operational phases

4.2.1 Early Phase

As described in Section 4.1, the spacecraft is launched using an Ariane 62. Commissioning is initiated one hour after launch.

4.2.2 Nominal operations

As per the mission requirements, the nominal science operations shall take 5 years. In the first two years, dedicated target observations will take place. Following that, EXODUS will perform a 1.5-year survey, confirming exoplanet suspects and candidates from other missions and ground-based instruments and making serendipitous discoveries. After the survey phase, a 6-month period will be dedicated to long-exposure target observations. Lastly, one year shall be dedicated to targets of opportunity.

Observation restrictions Mission requirements derived from the Ariane 62 fairing limit the sunshield size, which in turn limits the viewing angles. The strictest of them places a limit on the rotation of the spacecraft around the x-axis by the angle $\gamma \in (-10.5^\circ, 20^\circ)$. From this, we see that the entire sky be observed during the course of one year. We are provided by a continuous viewing zone

(CVZ) around the north ecliptic pole (NEP) and the southern ecliptic pole (SEP), in the regions of the ecliptic latitude of $\beta > 79.5^\circ$ and $\beta < -79.5^\circ$. Furthermore, we have an increased observability zone in the polar regions of $\beta \in (70^\circ, 79.5^\circ)$ and $\beta \in (-79.5^\circ, -70^\circ)$. The zone of lowest observability occurs at the ecliptic, where a given point can be observed for 30 days per year.

For a large part of our mission, the dedicated target observation and the survey phase, the observation program is structured into so-called cycles. A cycle consists of the observation of a fixed number of stars and their associated planetary systems.

Depending on the number of targets in a cycle and their angular separations, a total time for slewing arises. If we consider 2000 isotropically distributed targets, we obtain an average separation of 4.5° and an average slewing and settling time of 11 minutes based on JWST slew tables. Over one such cycle, taking about 240 days, the slew and settling time accounts for 15 days of the cycle. Three such cycles shall take place during the dedicated target observation phase.

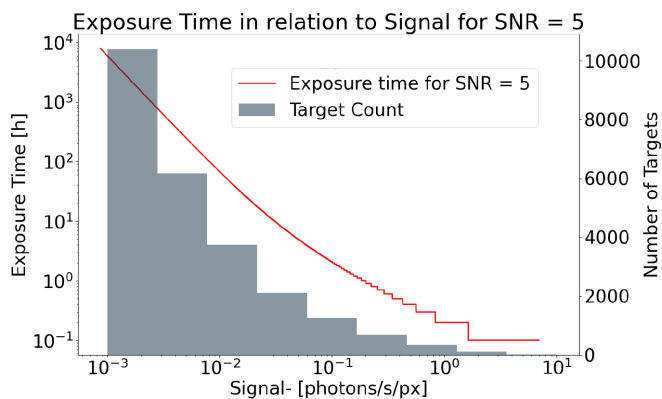


Figure 5: Number of observable targets.

Dedicated target observations From our own Monte Carlo simulations, which considered all the limitations of our systems, we find that 5600 exoplanets will be within our observational capabilities. Of them, around 60 exoplanets are expected to be observed around A-type stars, 130 around F-type stars, 320 around G-type stars, 680 around K-type stars, and 4400 around M-type stars, which form the majority of our sample.

Obvious targets for EXODUS will be provided by new exoplanets discovered from the expected Gaia data release, which by 2030 is expected to produce a sample of up to 15000 new exoplanets that have orbits on long orbital periods of approximately Jupiter mass and up, making them obvious targets for detection by EXODUS.

Furthermore, from the exoplanet population that has already been detected, 127 targets fall within our observation capabilities. These form targets for follow-up observations within the EXODUS mission. This target list contains well-known exoplanets such as the edge on β Pic, the bright 51 Eri, and the multiple system around HR 8799.

Based on the performance of the Teledyne HAWAII 4RG at a temperature of 120 K and the optical throughput of the system at 10%, we calculate that all our observations

will have a minimum SNR of 5, which is in line with our science requirements (see Figure 5).

Survey During the next 1.5 years, a large all-sky survey will be performed to discover new exoplanets. Suspected exoplanetary systems from Gaia and other missions will be observed, helping to further expand the explored region in the mass-period diagram.

Long exposure targets A set of interesting targets requiring exceptionally long (> 24 h) integration times has been separated from the principal target set, as it calls for a different observing strategy, optimizing for the total slewing and stabilization time. This set of targets has been given a separate six-month period.

Targets of opportunity The last part of the nominal science operations is dedicated to the observation of targets of opportunity. During this period, a large variety of objects shall be observed. An example of such a target are the forming exoplanets in the protoplanetary disk around the star PDS 70 (Müller et al., 2018). The EXODUS instrument is the perfect tool for protoplanetary disk observations and can be supported by ground-based instruments, such as VLT/SPHERE and VLTI, and radio observatories such as ALMA and LOFAR.

This phase will be also open to the entire astronomical community, as our instrument could provide important insights into various fields. As an example, we give observations of relativistic jets from galaxies, such as the one in M87.

4.2.3 Extended science operations

In the case of a surplus of expendables, science operations shall continue for as long as possible. Regular calls for proposals shall take place.

4.2.4 Decommissioning

A Δv budget of 10 m s^{-1} is allocated to inject the spacecraft from the Lissajous orbit around L_2 into a graveyard orbit. Later, the remaining fuel in the fuel tanks shall be emptied, the batteries shall be discharged and lastly, all systems shall shut down.

5 Spacecraft design

An overview of the subsystems implemented in the spacecraft is shown in Fig. 6. The following technical restrictions on the spacecraft acted as design drivers:

- The main dimensions of the mirrors came from the scientific requirements (minimum surface in order to collect the proper amount of photons), and also came from the optical design restrictions.
- Open telescope design in order to keep cool the instruments and also mirrors and structure without active heat removing system.
- Avoid or minimize the use of deployable mechanisms and structures
- Volume and mass restrictions from the launcher (Ariane 62)

The main parts and the structure as shown in Fig. 7:

- Optical system with 4 mirrors
- Instruments
- Thermal shield
- Service module
- Sunshield
- Propulsion with thrusters and propellant
- Communication

5.1 Structure

The optical system requires high pointing accuracy. In order to achieve this goal a rigid structure must be designed. Another key factor is the thermal behavior of the materials used and the mass, therefore a low thermal expansion coefficient and density are essential. One of the sensitive parts is the primary mirror. The deformation of the reflective surface must be of order a few tens of nanometers. Besides that, the mass also must be as low as possible in order to optimize the cost of the launch. Key parameters of possible mirror materials are shown in Table 3.

Another part is the relatively slender structure between the primary and secondary mirrors. The requirements are similar to the primary mirror. The main differences are the geometrical shape and dimensions. During the scientific phase, the relative position and angle error between the mirrors must be mitigated. In order to fulfill the technical expectations an extensive study will be essential.

5.2 ADCS and fine pointing

EXODUS utilizes a redundant configuration of four reaction wheels for three-axis attitude control. For an orbit around L₂, rotational disturbance may in large part be attributed to Solar Radiation Pressure (Wertz & Larson, 1999). Using a center-of-mass offset of 3 m to account for the geometrical constraints of the telescope, we find the angular momentum to be removed from the reaction wheel array per year to be 10 kNm.s. EXODUS carries 12 thrusters with a thrust of 20 N to ensure three-axis desaturation capability. For redundancy and to increase uptime, 6 thrusters are included.

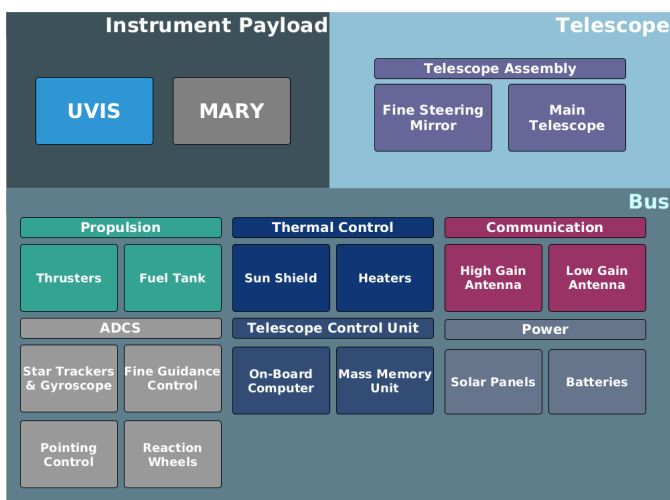


Figure 6: The subsystems of EXODUS.

The reaction wheel array provides 1" of pointing stability. Finer adjustments are achieved through high-frequency control of the Fast Steering Mirror (FSM). The UVIS visual channel acts as the main guiding channel for these measurements. The position is determined by the Instrument Software of the UVIS instrument, which will provide methods for Target Acquisition, Fine Pointing, and Guiding. Once the FSM has reached the limit in its range of motion it is reset by a small movement using the reaction wheels.

5.3 Thermal control

EXODUS is relying on a passive cooling design to cool down the spacecraft and its instruments. This is mainly done by using an open design, similar to JWST, to maximize the heat dissipation to the surrounding space. This, in combination with a seven-layer MLI (Multi-layer insulation) sunshield design, is providing the necessary temperature protection for the instruments. While the spacecraft-facing side of the outermost layer of the sunshield is at a temperature of 195 K, the temperature of the final layer of the sunshield is just below the target temperature of the instruments (80 K) at 76 K. The MLI is manufactured by Beyond Gravity and has an absorptance of 0.08 and emittance of 0.93¹.

Some of the subsystems are introducing heat into the system which is dissipated using 1.5 m² radiator panels connected to different parts of the spacecraft using heat pipes. Passive cooling is one of the system drivers in order to negate vibrations from the pumps in active cooling solutions and provide the best possible pointing accuracy.

5.4 Propulsion

The main propulsion system consists of 3 monopropellant thrusters with a thrust of 20 N each, manufactured by ArianeGroup. These thrusters will provide the necessary orbit correction authority with a thrust range from 7.9 N to 24.6 N and are proven in the space environment being aboard multiple missions like Herschel and Planck. The thrusters use a hydrazine propellant which decomposes and provides thrust when it hits the catalyst mesh in the nozzle section. The propulsion system is designed so that it produces as much thrust as possible, which is achieved with the placement of the thruster units.

5.5 Telescope Control Unit

The Telescope Control Unit consists of the On-board Computer (OBC) and the Mass Memory Unit (MMU). The OBC is the main component processing and distributing telecommands from the ground to the payload and collecting and processing science and housekeeping data from the payload.

The MMU is the main storage for science data for later transmission to the ground. In order to store the entire data generated over one day it needs at least 2.5 GB of storage.

¹beyondgravity.com

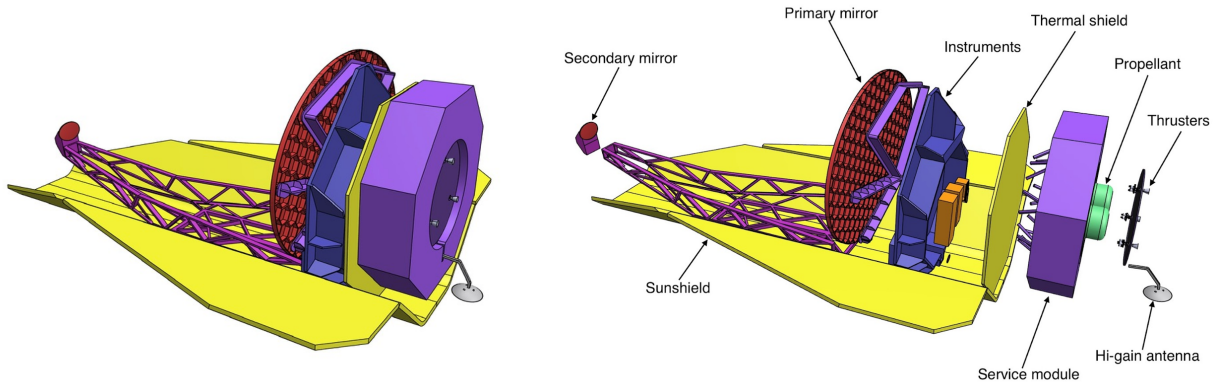


Figure 7: Left: Standard view of the spacecraft. Right: Exploded view of the spacecraft with descriptions of components.

Table 3: Parameters of considered materials, values taken from [Feinberg et al. \(2012\)](#).

Material	Density ρ [kg/m ³]	Young's Modulus E [GPa]	Specific Stiffness E/ρ [m]	Nominal Design Allowable Stress σ [MPa]	CTE at 293 K [ppm/K]	CTE at 40 K [ppm/K]
Borosilicate	2230	63	0.028	10	3.3	-3.2
Fused Silica	2200	73	0.033	10	0.5	-0.7
ULE	2210	68	0.031	10	0.03	-0.7
Zerodur	2530	91	0.036	10	0.05	-0.7
CVD SiC	3210	466	0.145	138	2.2	0.02
Reaction Bonded SiC	2910	360	0.124	69	2.4	0.02
O-30 Beryllium	1850	300	0.162	13	11	0.05
Aluminum	2700	70	0.026	69	23	2.5

5.6 Link budget and ground segment

The collection and distribution of the payload data obtained by EXODUS is an essential part of our mission. This will be sent to an antenna on Earth via radio communications. After that, a mission center must process and analyze the satellite payload data, and send it to a Science data center, where it will be studied. Finally, this payload data is sent to the Instrument teams in order to better control the pointing of the satellite and also archive the information for the science community.

As shown in Table 4, the data rate budget for EXODUS is predominantly driven by the science data that is generated by the payload and needs to be sent to ground. The estimates for the science data rates are based on the maximum sampling rate we expect during observations. The lossy data reduction is based on co-adding of 3 (MARY) to 10 (UVIS) frames and the lossless data compression rate is estimated with 2 for MARY and 2.5 for UVIS.

Table 4: Link budget overview.

Source	Gbits/day	Gbits/week+20% margin
ACOS	0.21	1.77
Housekeeping	0.06	0.57
MARY	18.47	155.23
UVIS	0.50	4.23
Total	19.36	162.77
Required		230.00

5.7 Power budget

The maximum power drawn by EXODUS is 1347 W - in the science mode of operation. This can be seen properly

in Table 5. The spacecraft is equipped with a VL51ES Battery by SAFT, with a nameplate energy of 9100 Wh and a nameplate capacity of 255 Ah. Main power generation will be done using solar panels, with a total generation of 1414 W. With these specifications, we can run the spacecraft in maximum current mode (science) for 6 hours and 45 minutes in case of temporal loss of power generation from solar panels.

5.8 Mass budget

The total mass budget for the space system, which includes the mass of the payload and spacecraft, is described in Table 6, with their respective margins.

6 Risks and rewards

6.1 Risk analysis

There are five prominent risks identified for the EXODUS missions: two mission risks and three development risks. A major risk is failure of the sunshield deployment, labelled with a possible likelihood and significant impact. If the unfolding mechanism does not function, the mission will have a pointing limitation due to reduced roll axes, primarily in the x-axis. Predetermined targets would become unavailable, requiring a change in the target selection strategy. Another mission risk is the failure of the adaptive optics, which is classed as a quite possible likelihood and catastrophic impact. This would have a severe impact on IR observations, but can be mitigated by regular testing of the design components.

In addition to mission risks, three development risks associated with technology development have been identified.

Table 5: Power budget overview of the spacecraft. P stand for power and M stands for margin.

Group	Component	Safe mode		Downlink		Science		Slewing	
		P [W]	P+M [W]	P [W]	P+M [W]	P [W]	P+M [W]	P [W]	P+M [W]
Payload	Instruments	100.0	120.0	100.0	120.0	400.0	480.0	100.0	120.0
	Fine guiding system	0.0	0.0	0.0	0.0	22.0	24.2	22.0	24.2
Communications	Transponder	55.0	60.5	55.0	60.5	11.0	12.1	55.0	60.5
	SSPA (power amplifier)	2.0	2.1	40.0	42.0	2.0	2.1	20.0	21.0
Electrical & Power	PCDU	50.0	52.5	50.0	52.5	50.0	52.5	50.0	52.5
Data Handling	Computer	15.0	16.5	15.0	16.5	15.0	16.5	15.0	16.5
	Memory	10.0	10.5	10.0	10.5	10.0	10.5	10.0	10.5
	Remote Interface Unit	15.0	16.5	15.0	16.5	15.0	16.5	15.0	16.5
Payload Thermal Control	Payload thermal	120.0	144.0	120.0	144.0	120.0	144.0	120.0	144.0
Propulsion Module	Propulsion	0.0	0.0	0.0	0.0	0.0	0.0	20.0	22.0
Service Module Thermal	Thermal control SVM	100.0	120.0	70.0	84.0	80.0	96.0	100.0	120.0
AOCS	AOCS Sensors & Electronics	25.0	27.5	25.0	27.5	25.0	27.5	25.0	27.5
	Reaction wheels	200.0	220.0	200.0	220.0	200.0	220.0	200.0	220.0
SVM Harness Losses (2%)	-	13.8	15.2	14.0	15.4	19.0	20.9	15.0	16.5
	Total	705.8	805.3	714.0	809.4	969.0	1122.8	767.0	871.7
	20% power margin	847.0	966.4	856.8	971.3	1162.8	1347.4	920.4	1046.1

Table 6: Mass budget overview of the spacecraft and its components.

Component	Mass [kg]	Margin	Mass + Marg.[kg]
Instruments	0.5	1.0	1.0
Adaptive optics:	120.7	1.0	241.4
Mirrors	533.3	0.2	640.0
Boom for M2	80.0	0.2	96.0
Solar Panels	5.6	0.05	5.9
Batteries	76	0.05	79.8
Antennas	10	0.05	10.5
Detector control unit	2.3	0.1	2.5
OBC + DPU	27.0	0.05	28.4
Thermal radiator	5.0	0.05	5.3
Sun shield	256.0	0.2	307.2
Fuel tanks + propulsion module	50.0	0.05	52.5
ADCS thruster	8.0	0.05	8.4
Orbit correction thrusters	2.0	0.05	2.1
Dry mass	1176.4		1480.8
5% harness	58.8	0.1	64.7
20% Structure	235.3	0.2	282.3
Dry mass	1470.4		1827.8
Dry mass+System margin		0.2	2193.4
Propellant	183.8	0.05	193.0
Wet mass			2386.4

In particular, development delay of the adaptive optics and coronagraph would result in a mission delay, which can be mitigated by rigorous design testing. Boom vibrations present a further development risk, having misalignment of the secondary mirror as an impact. Mock-up construction to examine structural behaviour is suggested for risk mitigation.

7 Cost

As illustrated in Table 7, the total cost of the mission is estimated to marginally exceed 1 billion euros. Mission development components constitute 50% of the total budget, ESA project 13%, mission operations 10%, science operations 5%, and the launcher 8.3%. A margin of approximately 10% is included to account for conceivable contingencies.

8 Descoping

To reduce spacecraft size, mass, and cost, a smaller cylindrical mirror could be used in place of an elliptical mirror. However, this would limit the observational distance and

Table 7: Cost analysis overview for the space mission.

	Cost (million euros)
Project team ESA	143
Development:	
-Service module	200
-Telescope	300
-Payload	50
Mission operations	110
Science operations	55
Contingency	128.7
Launcher	90
Total	1076.7

would narrow the scientific scope of the mission. Furthermore, a simplified adaptive optics system could be implemented, though this would limit the science case since observations would be restricted to larger targets with lower contrast.

9 Outreach

Scientific outputs from the mission should be disseminated widely, to a diverse audience. Therefore, it is important to establish a concurrent outreach programme for EXODUS, including a variety of events and activities for different target groups. In order to reach the public, we propose communication channels via social media, website development, live streams, and media interviews, as well as organising public science events (e.g. *exoplanet of the week*). In addition, development of a VR-platform would enable the public to become familiarised with the space environment and exoplanetary research in an engaging manner.

The programme would also include workshops for schools and universities, with adapted activities for the target group, including take-home material for students. For example, children could be offered painting books of space-related images to inspire and develop imagination. We will regularly downlink full-frame coronagraph images to generate captivating animations showing the movement of the exoplanets around the central star, both for artistic and scientific purposes. Finally, our work should also reach the scientific community to provide updates through con-

ferences and cooperation programmes, such as early-career researcher meetings.

10 Conclusions

In this report, we present a mission that will further push the boundaries of our knowledge of exoplanets. EXODUS will explore those areas of the exoplanet demographic that have so far gone unexplored: we will find giant planets on long orbital periods, we will detect the presence or absence of atmospheric escape, and we will further constrain the mechanisms of planetary evolution. This mission builds on the legacy of telescopes such as Gaia, the James Webb Telescope, and the Nancy Grace Roman Telescope, and will provide future generations new knowledge of exoplanets that will serve as a stepping stone to build upon.

Acknowledgements

We thank the organizers of the Summer School Alpbach, and all involved persons from the FFG, AustroSpace and ESA for their efforts in providing us with this unique opportunity and creating a welcoming and comfortable environment. We also want to thank all lecturers for their great presentations and for withstanding all of our tedious questioning. Additionally, we want to thank the tutors, especially Günter, Leonard, and Viktoria, even if she killed our mission once. Finally, we want to thank the Photons for finding their way to us in the end.

References

Auvergne, M., Bodin, P., Boissard, L., et al. 2009, *A&A*, 506, 411

Bagnasco, G., Kolm, M., Ferruit, P., et al. 2007, in *Cryogenic Optical Systems and Instruments XII*, ed. J. B. Heaney & L. G. Burriesci, Vol. 6692, International Society for Optics and Photonics (SPIE), 66920M

Benz, W., Broeg, C., Fortier, A., et al. 2021, *Experimental Astronomy*, 51, 109

Borucki, W. J., Koch, D., Basri, G., et al. 2010, *Science*, 327, 977

Brož, M., Wolf, M., & fyzikální fakulta, U. K. M. 2017, *Astronomická měření (MatfyzPress)*

Dos Santos, L. A., Vidotto, A. A., Vissapragada, S., et al. 2022, *A&A*, 659, A62

Feinberg, L. D., Dean, B. H., Hayden, W. L., et al. 2012, *Optical Engineering*, 51, 011006

Fulton, B. J., Petigura, E. A., Howard, A. W., et al. 2017, *AJ*, 154, 109

Gaia Collaboration, Prusti, T., de Bruijne, J. H. J., et al. 2016, *A&A*, 595, A1

Gardner, J. P., Mather, J. C., Clampin, M., et al. 2006, *SSR*, 123, 485

Gaudi, B. S., Seager, S., Mennesson, B., et al. 2020, arXiv e-prints, arXiv:2001.06683

Ginzburg, S., Schlichting, H. E., & Sari, R. 2018, *MNRAS*, 476, 759

Guerri, G., Daban, J.-B., Robbe-Dubois, S., et al. 2011, *Experimental Astronomy*, 30, 59

Hechler, M. & Yanez, A. 2004, *Herschel/Planck Consolidated Report on Mission Analysis*

Lagier, R. 2021, *Ariane 6 User's Manual. Issue 2 Revision 0*

Lammer, H., Selsis, F., Ribas, I., et al. 2003, *ApJ*, 598, L121

Lopez, E., Airapetian, V., Christiansen, J., et al. 2019, *BAAS*, 51, 522

Lyot, M. B. 1939, *Monthly Notices of the Royal Astronomical Society*, 99, 580

Mayor, M., Pepe, F., Queloz, D., et al. 2003, *The Messenger*, 114, 20

Mayor, M. & Queloz, D. 1995, *Nature*, 378, 355

Müller, A., Keppler, M., Henning, T., et al. 2018, *A&A*, 617, L2

Navarro, R., López, J. L., Díaz, J. A., & Sinusía, E. P. 2014, *Opt. Express*, 22, 21263

Oklopčić, A. 2019, *ApJ*, 881, 133

Oklopčić, A. & Hirata, C. M. 2018, *ApJ*, 855, L11

Owen, J. E. & Wu, Y. 2013, *ApJ*, 775, 105

Pepe, F., Cristiani, S., Rebolo, R., et al. 2021, *A&A*, 645, A96

Perryman, M., Hartman, J., Bakos, G. Á., & Lindgren, L. 2014, *ApJ*, 797, 14

Platt, B. C. & Shack, R. 2001, *History and principles of Shack-Hartmann wavefront sensing*

Pollacco, D. L., Skillen, I., Collier Cameron, A., et al. 2006, *PASP*, 118, 1407

Prusti, T. 2012, *Astronomische Nachrichten*, 333, 453

Rauer, H., Catala, C., Aerts, C., et al. 2014, *Experimental Astronomy*, 38, 249

Ricker, G. R., Winn, J. N., Vanderspek, R., et al. 2015a, *Journal of Astronomical Telescopes, Instruments, and Systems*, 1, 014003

Ricker, G. R., Winn, J. N., Vanderspek, R., et al. 2015b, *Journal of Astronomical Telescopes, Instruments, and Systems*, 1, 014003

Ruane, G. J. & Swartzlander, G. A. 2013, *Appl. Opt.*, 52, 171

Spake, J. J., Sing, D. K., Evans, T. M., et al. 2018a, *Nature*, 557, 68

Spake, J. J., Sing, D. K., Evans, T. M., et al. 2018b, *Nature*, 557, 68

Spergel, D., Gehrels, N., Baltay, C., et al. 2015, arXiv e-prints, arXiv:1503.03757

The LUVUOIR Team. 2019, arXiv e-prints, arXiv:1912.06219

Tian, F. 2015, *Annual Review of Earth and Planetary Sciences*, 43, 459

Tinetti, G., Drossart, P., Eccleston, P., et al. 2018, *Experimental Astronomy*, 46, 135

Wertz, J. R. & Larson, W. J. 1999, *Space mission analysis and design*, Vol. 8 (Springer)

Wheatley, P. J., West, R. G., Goad, M. R., et al. 2018, *MNRAS*, 475, 4476

Wordsworth, R. & Kreidberg, L. 2022, *ARA&A*, 60, 159

Wordsworth, R. D., Forget, F., Selsis, F., et al. 2011, *ApJ*, 733, L48

Zernike, v. F. 1934, *Physica*, 1, 689